Materials Research. 2023; 26: e20220487
DOI: https://doi.org/10.1590/1980-5373-MR-2022-0487

Thermoelectric Properties of $Ca_3Co_4O_9$ Using Microwave Synthesis and Sintering

Ana Clara de Paula Lima[a], *Daniel Thomazini*[a]*, *Adilson Luiz Chinelatto*[b], *Maria Virginia Gelfuso*[a]

[a]*Universidade Federal de Itajubá (UNIFEI), Grupo de Desenvolvimento de Materiais Funcionais (GDMaF), 37500-903, Itajubá, MG, Brasil.*
[b]*Universidade Estadual de Ponta Grossa (UEPG), 84010-330, Ponta Grossa, PR, Brasil.*

Received: November 17, 2022; Revised: April 13, 2023; Accepted: April 19, 2023

$Ca_3Co_4O_9$ powders and ceramics were synthesized and sintered using microwave-assisted heating method.Another batch of powders was calcined by the conventional heating method and this powder was used to produce ceramics sintered by microwave sintering aiming to compare with those prepared by microwave method. The formation of the phases based on calcination method and time was assessed by X-ray diffractometry. The synthesis and sintering methods affected various properties of the ceramics, including grain size, density, phase amount, Seebeck coefficient, thermal conductivity and electrical conductivity. Microwave heating method reduced the time required for the powder synthesis and sintering of ceramics. Ceramics produced using powder obtained by the conventional method presented Figure of Merit (ZT) values of approximately 0.04. However, these values were reduced for the ceramics produced by microwave heating reaching a value of about 0.02. The evaluation of the thermoelectric properties of the $Ca_3Co_4O_9$ ceramics suggests that the main issue to enhance the Figure of Merit of the CCO ceramics is related to density and $Ca_3Co_4O_9$ phase amount present in the ceramics.

Keywords: *Microwave processing, thermoelectric ceramics, electrical conductivity, thermal conductivity.*

1. Introduction

Thermoelectric materials have gained attention as a promising alternative method to produce electrical energy from harvested waste heat from thermal systems. The thermoelectric conversion of these materials depends on the Seebeck effect, and its efficiency is estimated using the Figure of Merit (ZT), expressed as $ZT = S^2\sigma T/\kappa$, where σ represents electrical conductivity, S is the Seebeck coefficient, κ is the thermal conductivity, and T is absolute temperature[1]. From combination of high Seebeck coefficient, electrical conductivity and low thermal conductivity values, ZT values can be significatively expressive resulting in higher thermoelectric conversion efficiency[2].

$Ca_3Co_4O_9$ (CCO) ceramics have attracted significant research interest[3], mainly due to their high chemical resistance and thermal stability at high temperatures[4]. Moreover, CCO ceramics are environmentally friendly, involving low temperatures for its production, and exhibit no toxicity[5], making this cobaltite oxide a significant alternative for thermoelectric applications[6]. The layered structure of $Ca_3Co_4O_9$ consists of a conductive layer, CoO_2^{2+}, and an insulator layer, $Ca_2CoO_3^{2-}$. The crystal structure of $Ca_3Co_4O_9$ possesses a p-type semiconducting behavior, occuring as the function of changing from Co^{3+} to Co^{4+} in the CoO_2^{2+} layer[7].

According to the research reported by Annamalai et al.[8], most of the studies of calcium cobaltite are focused on the conventional sintering method, the solid-state, and the sol-gel reaction sintering process, which are effective methods to obtain $Ca_3Co_4O_9$ ceramics. However, according to Miyazawa et al.[9], there is a lack of systematic studies of the microwave method used to synthesize and sinter calcium cobaltite.

The microwave-assisted heating method is selectivity in energy transfer, promoting higher heating rates, contributing to a very short time for the reactions and sintering, favoring reaction yields and structural uniformity of products, and fast densification resulting from the enhancement of diffusion processes[9]. During the incidence of the microwave radiation in the material, an intense electromagnetic field concentrates around the sample[10], interacting with the surface ions, promoting an effective ionization of the particles and rising the ions' diffusion[11]. Considering that the microwave heating method is based on the absorption of this electromagnetic radiation, it can promote an acceleration of the synthesis and densification of this material. Therefore, this method presents many advantages compared to those based on conventional, such as higher energy efficiency, higher post-sintering density, and lower sintering temperatures[12], making it a suitable alternative for processing thermoelectric ceramics.

This work is focused on obtaining $Ca_3Co_4O_9$ ceramics prepared from powder calcined and sintered using microwave-assisted heating method. The aim is to investigate the influence of this method on synthesis, densification, microstructure evolution, electrical, thermal, and thermoelectric properties of these ceramics and compare its properties to those prepared from powder calcined by the conventional resistive method.

*e-mail: thomazini@unifei.edu.br

2. Experimental Procedure

Initially, the raw precursors, $CaCO_3$ (Sigma-Aldrich, 99.0%) and $Co(NO_3).6H_2O$ (Sigma-Aldrich, 95.0%), were mixed in a 3:4 stoichiometric ratios, respectively, to produce the $Ca_3Co_4O_9$ (CCO) powders. The reagents were mixed and stirred magnetically in an open beaker with reverse osmosis water for 60 minutes and subsequently dried in atmospheric air for 24 h at 70 °C. The dried mixture powder was deagglomerated and sieved through #320, and divided in quotas to be calcinated by two routes: one by microwave-assisted heating method (MW) using a modified domestic microwave furnace with SiC as a microwave susceptor, and the other by conventional resistive heating, or conventional calcination process, named solid-state reaction (SSR).

The conventional calcination process was carried out in a conventional electrical furnace for 120 minutes at 900 °C (CCO120SSR) with a heating rate of 10 °C/min in atmospheric air, based on a previous study[5]. Then, samples of the calcined powder were uniaxially pressed in a metallic mold applying 350 MPa at room temperature into discs with a diameter of 12 mm and a thickness of 1 mm. After, the samples were sintered in a microwave furnace at 900 ºC for 30 minutes (CCO120SSR-30MW) and 60 minutes (CCO120SSR-60MW), both at 250 ºC/min. The sintering process was performed in atmospheric air.

In the microwave-assisted calcination route, the mixture powder were heated in a microwave furnace at 900 °C for 15 min (CCO15MW), 30 min (CCO30MW), and 60 min (CCO60MW) in atmospheric air. Then, the calcined powders were uniaxially pressed at 350 MPa into discs shape with a diameter of 12 mm and a thickness of 1 mm. The samples were sintered in the microwave furnace at 900 °C for 30 min (CCO60MW-30MW) and 60 min (CCO60MW-60MW). The heating rate in this route was maintained at 250 ºC/min in atmospheric air.

Relative densities were calculated based on Archimedes' principle using water as a fluid and adopting the value of 4.67 g/cm^3 as theoretical density for $Ca_3Co_4O_9$. The crystalline phases of calcined powders and ceramics were identified through X-ray diffraction analysis (XRD – Shimadzu 6000) with Cu-Kα radiation (λ = 1.5405 Å), an integration time of 0.5 s, and a step size of 0.02 °. High Score Plus software and ICDD with PDF-4 library and COD databases were used to confirm the crystalline phases, and the Rietveld method was used for semi-quantification of phases. All fitted XRD patterns had $R_{factors}$ (R_{exp}, R_p, and R_{wp}) of less than 10%.

The ceramic densities (ρ) were calculated by the ratio between its mass and volume. The theoretical density of each sample was determined by applying the rule of mixtures, which considers the crystalline phase amount and density of each phase. For $Ca_3Co_4O_9$[13], $Ca_3Co_2O_6$ and Co_3O_4 phases, densities of 4.67 g/cm^3, 4.50 g/cm^3 [ICOD #021-0138], and 6.05 g/cm^3 [ICOD #042-1467], respectively, were adopted. These values were used to calculate $\rho_{relative}$. The volumetric apparent open porosity of the ceramics was calculated using the equation $\%P_o = 100\%*(M_w-M_d)/(M_w-M_i)$, where M_w, M_d, and M_i represent the wet, dry and immersed mass of the ceramic bodies, respectively. Archimedes' principle using water as a fluid was used to measure M_i. Close porosity was calculated from $\%P_c = \%P_t - \%P_o$, where the total porosity of the ceramics was obtained from $\%P_t = 100\% - \rho_{relative}$.

Images of the calcined powders and ceramic surfaces were examined using scanning electron microscopy (SEM – Phenom ProX) using a BSE detector. The average size and standard deviation of 100 powder particles and 100 ceramics grains, respectively, were measured using ImageJ software[14] based on the SEM images. To visualize the SEM images of the powders, they were dispersed in isopropanol with the aid of ultrasound and deposited on the sample holder.

The thermal conductivities (κ) (Netzsch LFA-457) of the ceramics were measured in the range of 50 to 600 °C under a nitrogen atmosphere to protect the graphite coating on samples. The 4-probe DC electrical conductivity (σ) and Seebeck coefficient (S) measurements (SB-01, WT Industria) were conducted from 50 °C to 600 °C at a heating rate of 1 °C/min in atmospheric air.

3. Results and Discussion

Figure 1a shows the X-ray diffractions patterns, and Figure 1b the semi-quantification of the crystalline phase present in the conventional and the microwave calcined powders. The presence of crystalline phases for $Ca_3Co_4O_9$ [ICOD #21-0139] is noticed, followed by the formation of secondary phases such as $Ca_3Co_2O_6$ [ICOD #021-0138] and Co_3O_4 [ICOD #042-1467]. The formation of $Ca_3Co_2O_6$ and Co_3O_4 phases can occur due to the poor oxygen atmosphere at high temperatures[15], which is evidenced by presence of some peaks related to these secondary phases.

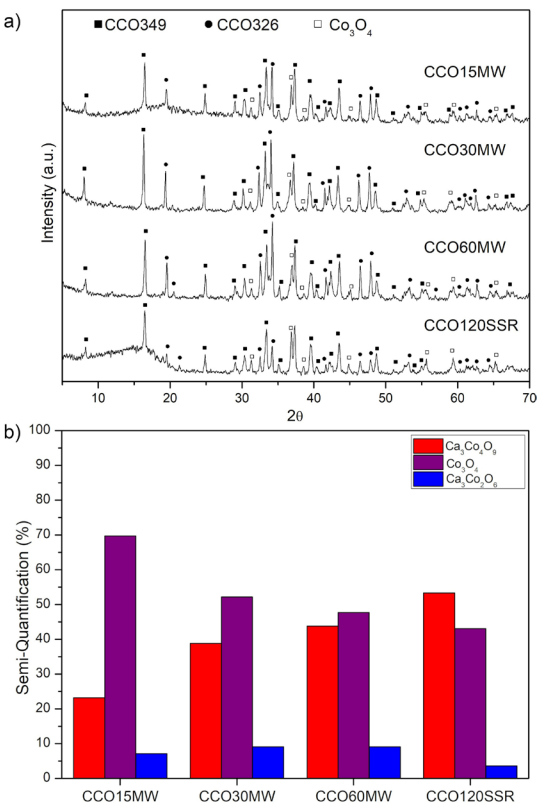

Figure 1. (a) XRD patterns of CCO15MW, CCO30MW, CCO60MW, and CCO120SSR-30MW $Ca_3Co_4O_9$ powders. (b) – Powders' semi-quantification by using Rietveld refinement.

XRD patterns for microwave-calcined powders revealed that even with only 15 minutes, it was able to consolidate about 23% of the $Ca_3Co_4O_9$ phase. Diffraction peaks at 8.18°, 16.43°, and 33.33° are evident from the $Ca_3Co_4O_9$ phase, but secondary phases also are present, which can be attributed to the shorter hold durations for calcination and restricted oxygen atmosphere. After 60 minutes of calcination, about 44% of the $Ca_3Co_4O_9$ phase was obtained, but for 120 minutes in conventional calcination, 53% of the $Ca_3Co_4O_9$ phase was produced. Considering powder calcined in microwave process, all XRD patterns indicate the Co_3O_4 phase as the main compound, followed by $Ca_3Co_4O_9$, and then $Ca_3Co_2O_6$ phases, but all of them became less evident with sintering time. Observing Figure 1b, the amount of Co_3O_4 and $Ca_3Co_2O_6$ phases decreases with increasing calcination time, while the amount of the $Ca_3Co_4O_9$ phase increases. Additionally, comparing the values of the main phase obtained for the CCO60MW and CCO120SSR, the former presented a very expressive result, considering that one hour less calcination was spent.

Figure 2a presents the XRD patterns for ceramics sintered using microwave irradiation. $Ca_3Co_4O_9$ peaks can be observed, which may be related to the promising values of the thermoelectric properties obtained through this method. Moreover, the CCO60MW-60MW sample exhibits the highest amount of the CCO phase. These results are relevant to enhancing the thermoelectric properties; thus, reducing the amount of Co_3O_4 and $Ca_3Co_2O_6$ induces an increase in the thermoelectric properties of the sintered ceramics[16]. $Ca_3Co_4O_9$ ceramics obtained through the conventional method at 800 °C[17], 850 °C[16], or 920 °C[18], also presented secondary phases, such as $Ca_3Co_2O_6$ and Co_3O_4, mainly due to oxygen deficiency, as previously discussed. Additionally, semi-quantification results of CCO ceramics are indicated in Figure 2b. The CCO60MW-60MW ceramic, starting from the powder with 44% of the $Ca_3Co_4O_9$ phase, exhibited the most effective result in terms of the main phase ($Ca_3Co_4O_9$), achieving about 82% of its composition. On the other hand, the CCO120SSR-60MW ceramic presented about 78% of the $Ca_3Co_4O_9$ phase, even starting from the powder containing 53% of this phase. So, the microwave calcination was able to significantly increase the amount of $Ca_3Co_4O_9$ phase in the CCO powder and also subsequently in the sintered ceramics.

Figure 3 displays the SEM micrographs of the CCO powders and ceramics, namely CCO120SSR (Figure 3a), CCO60MW (Figure 3b), CCO120SSR-30MW (Figure 3c), CCO120SSR-60MW (Figure 3d), CCO60MW-30MW (Figure 3e), and CCO60MW-60MW (Figure 3f). The CCO60MW powder exhibited particles with more uniform distribution and lower particle coarsening compared to the CCO120SSR powder, as the ions' diffusivity was promoted by the surrounded electromagnetic field from microwave radiation[11]. The particle size of the powders, grain size, and relative densities of the ceramics are presented in Table 1, revealing the influence of the different methods used to produce the CCO ceramics.

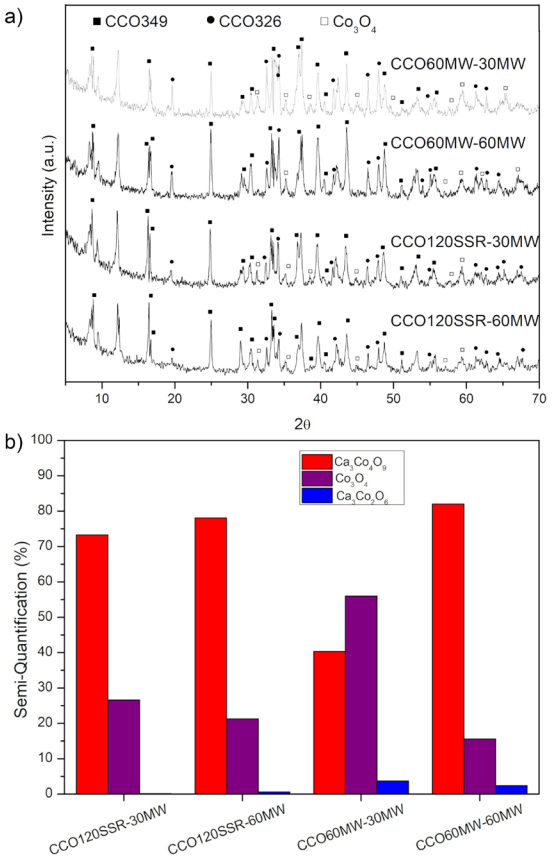

Figure 2. (a) XRD patterns of CCO60MW-30MW, CCO60MW-60MW, CCO120SSR-30MW and CCO120SSR-60MW ceramics. (b) Ceramics' semi-quantification by using Rietveld refinement.

Table 1. Average particle and grain size, absolute (ρ) and relative density ($\rho_{relative}$), apparent open (%P_o) and close (%P_c) porosity of the samples.

Sample	Particle/Grain Size (μm)	ρ(g/cm³) [$\rho_{relative}$(%)]	%P_o (%)	%P_c (%)
CCO15MW	1.09 ± 0.32	-	-	
CCO30MW	1.04 ± 0.33	-	-	
CCO60MW	0.95 ± 0.39	-	-	
CCO120SSR	1.06 ± 0.41	-	-	
CCO120SSR-30MW	1.06 ± 0.35	2.83 [56.4%]	43.4	0.2
CCO120SSR-60MW	1.15 ± 0.33	2.67 [53.8%]	43.1	3.1
CCO60MW-30MW	1.09 ± 0.28	2.06 [37.8%]	47.6	14.6
CCO60MW-60MW	1.13 ± 0.42	2.10 [43.0%]	45.8	11.2

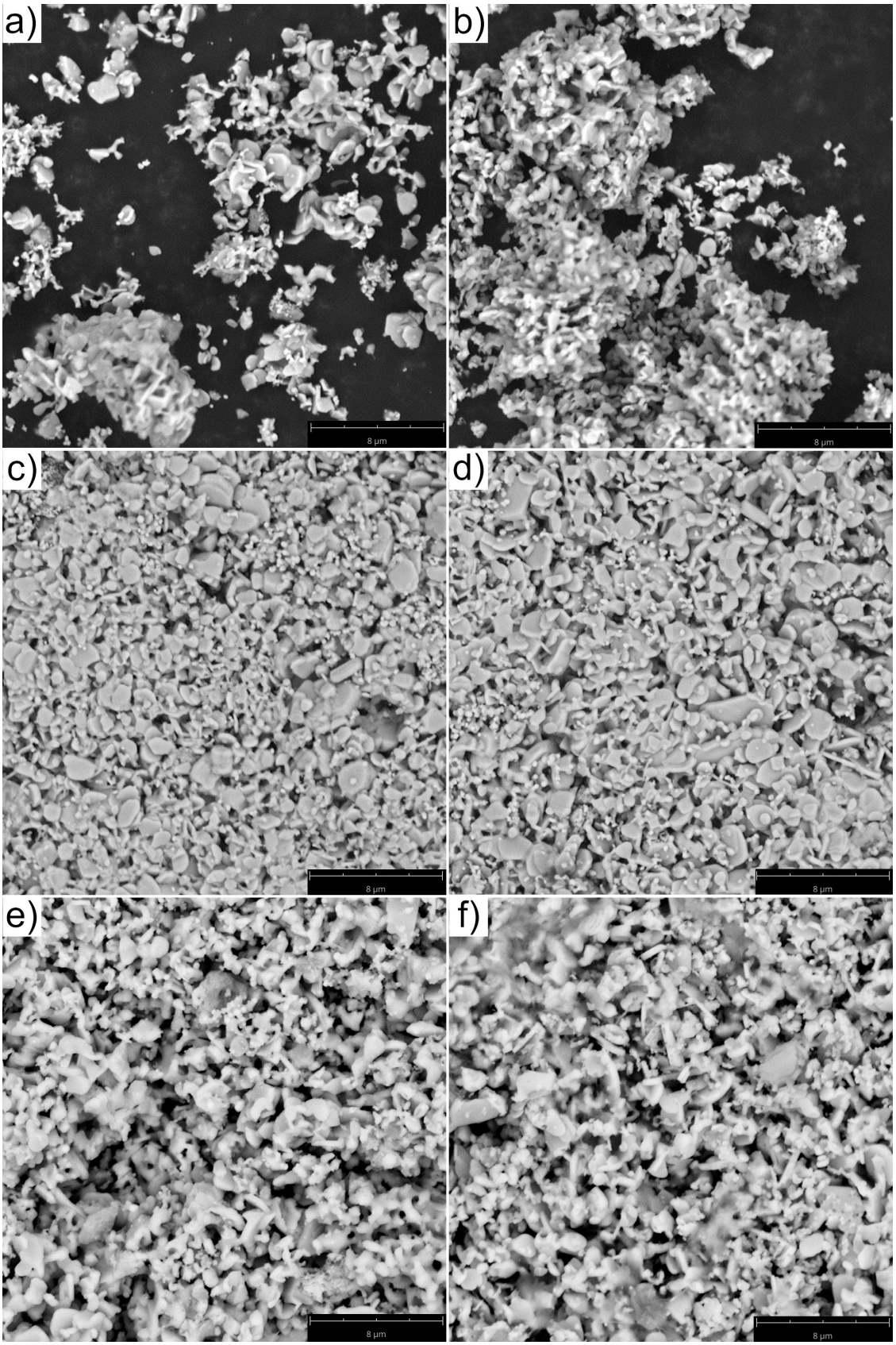

Figure 3. SEM images of $Ca_3Co_4O_9$ samples: (a) CCO120SSR, (b) CCO60MW, (c) CCO120SSR-30MW, (d) CCO120SSR-60MW, (e) CCO60MW-30MW and (f) CCO60MW-60MW.

As expected, a separately analysis of both groups of ceramics, one produced by conventional calcination process (CCO120SSR) and the other using microwave calcination process (CCO60MW), showed grain growth. to CCO120SSR-60MW ceramic (1.15 ± 0.33 μm) presenting a slightly higher average grain size than CCO120SSR-30MW (1.06 ± 0.35 μm), despite the deviation. The same behavior can be observed in the ceramic produced from the group calcined using microwave irradiation, with CCO60MW-30MW showing 1.09 ± 0.28 μm, while CCO60MW-60MW presented values about 1.13 ± 0.42 μm. However, a comparison of both groups showed that sintering holding time caused a small increase in the average grain size. CCO120SSR-30MW ceramic did not have a significant increase in its average grain size, while CCO120SSR-60MW obtained an increase compared to the initial particle size, thus reinforcing the microstructural effects of using microwave sintering. Moreover, the temperature and time of sintering are significant factors for the microstructure, as reported in the literature[5,19,20]. CCO ceramics produced by different methods result in ceramics with higher grain size than the microwave sintering. Ceramics obtained by solid-state reaction[5], sintered by 6 h, presented grain size of 1.39 μm and 58% of relative density, while ceramics produced by chemical route[15], sintered by 12 h, reached a grain size of 1.21 μm and a relative density of 66%. In both cases, even with longer holding sintering time, it was not effective to enhance the density or grain size of those ceramics. The higher porosity presented by CCO60MW-30MW ceramic indicates lower densification when compared to the other sintered samples (CCO60MW-60MW). CCO ceramics are well-known to present low densification due to their particles and grain morphology. A similar effect can also be observed in microwave-sintered ceramics. Moreover, evaluating the porosity of the ceramics, those produced from SSR powder predominantly presents open porosity, while ceramics obtained from MW powder present from 75.5 to 80.0% of open porosity relative to total porosity. The main difference between both powders is the amount of phases. CCO60MW powder present higher Co_3O_4 amount, phase which present high microwave radiation absorption[21], and melting temperature of 895 °C[22], close to sintering temperature, so, these issues may favor the liquid phase formation that favor to close porosity.

Figure 4 presents the temperature dependence of the electrical conductivity (σ) of the ceramics exhibiting semiconducting behavior[23]. The behavior of σ for SSR ceramics was similar, with CCO120SSR-60MW ceramic presenting slightly higher values at 2018 S/m, while CCO120SSR-30MW presented 1895 S/m, both at 600 °C. These values are similar to those obtained using conventional methods[5,24]. These results can be attributed to the larger grain size, which presents lower grain boundaries that act as scattering centers to charge carriers due to the higher sintering time, favoring the electrical conductivity[15]. The lowest electrical conductivity value of 767 S/m was obtained for CCO60MW-30MW ceramic calcined by microwave irradiation, which contained smaller amounts of the main thermoelectric $Ca_3Co_4O_9$ phase, as shown in Figure 2b. Although both CCO120SSR-60MW and CCO60MW-60MW ceramics have similar grain size and CCO phase amount, the latter's electrical conductivity is almost half, and its relative density is the smaller. The porosity effect can contribute to scattering the charge carriers at grain boundaries[25] and negatively interfere on σ values, making it the main issue in reducing the electrical conductivity of the CCO60MW-60MW ceramic.

Figure 5 illustrates the electronic (κ_e) and lattice contributions ($\kappa_{lattice}$) to the thermal conductivity of the sintered ceramics between 50-600 °C. The electronic thermal conductivity (κ_e), which is attributed to the electronic contribution, can be associated with electrical conductivity by Wiedemann−Franz law[26], which states that $\kappa_e = L \times \sigma \times T$, where L is the Lorenz Number (1.84×10^{-8} $W\Omega K^{-1}$) for a non-degenerate semiconductor based on the Seebeck values[27]. The $\kappa_{lattice}$ can be estimated as the difference between total κ and the electronic component, $\kappa_{lattice} = \kappa - \kappa_e$. Note that as T increases, thermal conductivity decreases, thus the $\kappa_{lattice}$ contribution in $Ca_3Co_4O_9$ materials is more dominant than the κ_e contribution[4], as expected for semiconducting oxide ceramics[28]. The lowest κ values at 600 °C were observed in the CCO60MW-30MW and CCO60MW-60MW ceramics, at 0.713 and 0.768 W/mK, respectively.

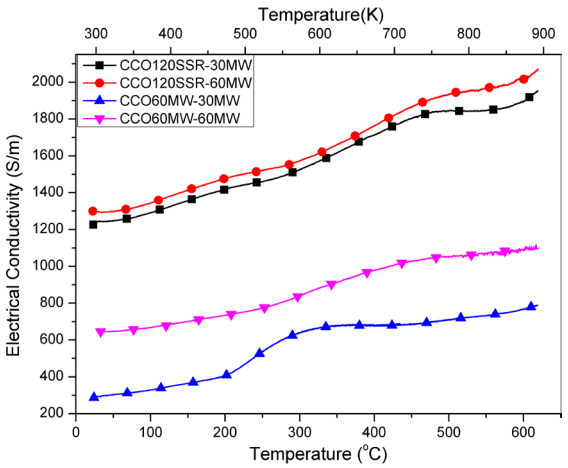

Figure 4. Temperature dependence on electrical conductivity (σ) of the ceramics.

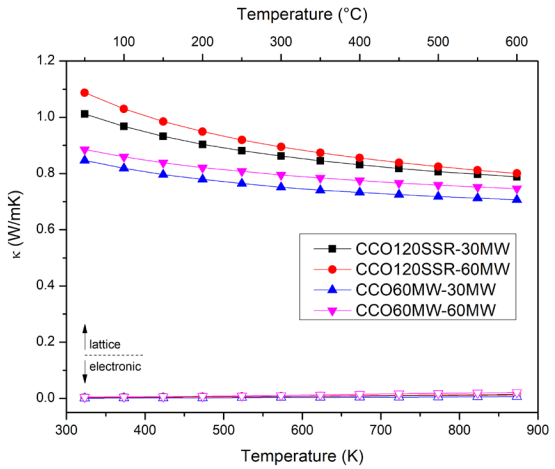

Figure 5. Temperature dependence on lattice and electronic thermal conductivity of the ceramics.

The highest κ values were produced by CCO120SSR-60MW, at 0.815 and CCO120SSR-30MW ceramics, at 0.801 W/mK, both at 600 °C. Ceramics calcined using microwave heating showed slightly lower $\kappa_{lattice}$ values compared to ceramics calcined produced from the conventional process. This behavior could be explained by an increasing in the amount of interface phonon scattering at grain boundaries, reducing the phonon mean free path and hence, decreasing $\kappa_{lattice}$[25]. Additionally, CCO60MW-60MW and CCO60MW-30MW ceramics exhibit the highest porosity, 45.8 and 47.6%, respectively, which reduced the mean free path of some phonon modes and contributed to a significant decrement in the κ values[29].

The temperature dependence on the Seebeck coefficient of all the ceramics is displayed in Figure 6. The results show a positive Seebeck coefficient for the ceramics, indicating that $Ca_3Co_4O_9$ is a p-type semiconductor, which is consistent with the literature[30,31]. The cobaltite structures contain CoO_2^{2+} planes, which provide a path for p-type electronic conduction and are separated by a $Ca_2CoO_3^{2-}$ layer, leading to the formation of a rock-salt type structure[32]. This structure contributes to interesting values of the Seebeck coefficient. All the samples exhibit the same trend for the Seebeck coefficient values, which increase with the temperature. The highest Seebeck values were obtained for the ceramics CCO120SSR-30MW with 139.8 uV/K and CCO60MW-60MW with 138.1 uV/K, both at 600 °C. The lowest value was 120.9 uV/K at 600 °C for the CCO60MW-30MW, and this behavior can be due to the moderate quantification of the major phase in the ceramic, evidenced by the Co_3O_4 phase, which tends to decompose and favor the formation of the $Ca_3Co_4O_9$. Furthermore, no significant variation was observed as the temperature increased and is following the results reported by Annamalai et al.[8]. So, in this case, it would be noted the Seebeck coefficient is insensitive to both sintering methods used in the present study. The literature review supports our results that the Seebeck coefficient is insensitive to the sintering technique, temperature, and bulk density[33]. CCO ceramics processed by conventional sintering, Spark Plasma Sintering reported nearly the same values of Seebeck coefficient with a maximum value of 170 μV/K at 527 °C[34].

Figure 7 displays the influence of process parameters on the average grain size, density, and the thermoelectric properties of the $Ca_3Co_4O_9$-based ceramics at 600 °C. It is clear that these properties are affected by the processing. Ceramics with larger grain sizes have smaller areas of grain boundaries, hence reducing phonon scattering in the grain boundary interface, contributing to the enhanced thermal conductivity of the material, as observed for the CCO120SSR-60MW ceramic[25]. It is noted that the relative density slight increases and the apparent porosity decreases with sintering time. Therefore, the ceramic with the highest relative density value is the CCO120SSR-30MW, presenting 56.4%. As expected, increasing the sintering temperature results in increased densification and stabilized porosity of the CCO ceramics. However, ceramics did not enhance density values, analogous to other studies related to microwave sintering. Miyazawa et al.[9] obtained CCO ceramics with 81% relative density using microwave sintering. Annamalai et al.[8] reported about 96% of relative density for samples obtained by microwave reactive sintering. Both used heating rates lower than 100 ºC/min, which is lower than that used in this study (250 ºC/min). Even in literature, the microwave sintering approach is used to produce other ceramics as ferrites[11], with a high heating rate and this parameter also depends on the sample mass. These results suggest a dependence of rate heating of microwave sintering encouraging future studies. The enhancement of the σ in the CCO60MW-60MW is mainly due to the $Ca_3Co_4O_9$ phase being strongly consolidated and the decrement in the Co_3O_4 formation, as shown by XRD results.

Figure 8 display the temperature dependence of ZT values for the ceramics obtained at different parameters.

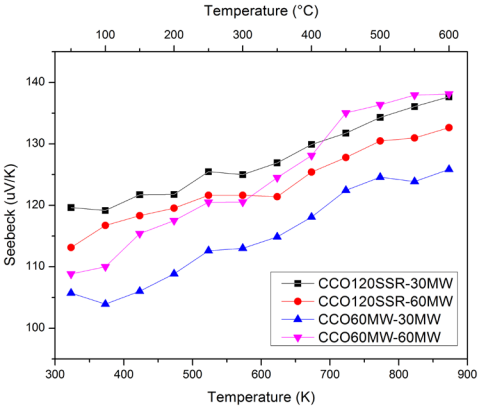

Figure 6. Temperature dependence on Seebeck coefficient (S) of the ceramics.

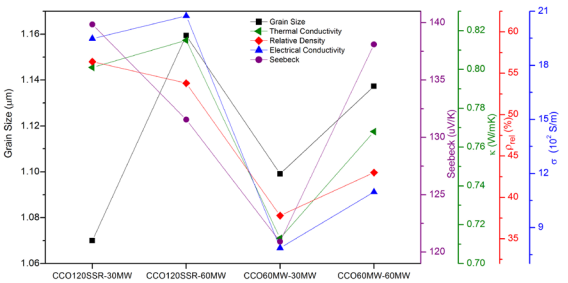

Figure 7. Influence of grain size on the thermoelectric properties of $Ca_3Co_4O_9$ ceramics at 600 °C.

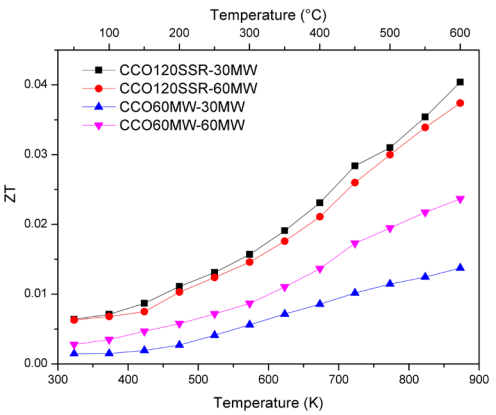

Figure 8. ZT values at different temperatures of $Ca_3Co_4O_9$ ceramics.

The highest value was obtained in to ceramics produced in conventional calcination. This lowest value was obtained due to the higher porosity attributed to the sample, hence the σ is reduced, as discussed above. The ceramic powders calcined in the conventional furnace produced ceramics with similar ZT values, CCO120SSR-30MW and CCO120SSR-60MW with 0.037 and 0.040, respectively, which can be due to their similar density values, which is following with the literature[5,8,24]. The increase in the electrical conductivity of conventional calcined powder significantly increased the ZT values. The grain size barely changed between the ceramics, but the increase in the CCO phase amount aided by density could enhance the ZT values of these ceramics.

4. Conclusion

Microwave-assisted heating was used to calcination and sintering to produce $Ca_3Co_4O_9$ ceramics. The results showed that microwave calcination was able to significantly increase the amount of the $Ca_3Co_4O_9$ phase in the CCO powder and subsequently in the sintered ceramics. The XRD patterns revealed the presence of crystalline phases for $Ca_3Co_4O_9$, followed by the formations of secondary phases as $Ca_3Co_2O_6$ and Co_3O_4. The SEM micrographs of the CCO powders and ceramics showed that the CCO60MW powder exhibited particles with a more uniform distribution and lower particle coarsening compared to the CCO120SSR powder. Ceramics produced by conventional calcination were found to have higher densification and $Ca_3Co_4O_9$ phase amount than samples produced by microwave heating. Overall, the study demonstrated the potential of microwave calcination for the synthesis of $Ca_3Co_4O_9$ ceramics with improved thermoelectric properties.

5. Acknowledgments

The authors of this study would like thanks to CNPq (National Council for Scientific and Technological Development of Brazil - 307783/2020-0) and FAPEMIG (Minas Gerais State Foundation of Support to the Research – APQ-01856-22) for the financial grant.

6. References

1. Sanchaniya J, Pathak B, Gagliya K, Joshi US. Electrical transport and thermoelectric study of $Ca_3Co_4O_9$ ceramics. Mater Today Proc. 2021 [cited 2023 Apr 19];47:665-7. https://linkinghub.elsevier.com/retrieve/pii/S2214785320398321.
2. Ruan C, Song H, Fan M, Hao H, Liu S. Enhancement of $Ca_3Co_4O_{9+\delta}$ thermoelectric properties by dispersing SiC nanoparticles. Ceram Int. 2021;47(5):6548-53.
3. Xu K, Liu H. Introducing Ta_2O_5 nanoparticles into $Ca_3Co_4O_9$ matrix for increased thermoelectric property through phonon scattering. Ceram Int. 2020;46(16):25783-8.
4. Kenfaui D, Lenoir B, Chateigner D, Ouladdiaf B, Gomina M, Noudem JG. Development of multilayer textured $Ca_3Co_4O_9$ materials for thermoelectric generators: influence of the anisotropy on the transport properties. J Eur Ceram Soc. 2012 [cited 2012 May 21];32(10):2405-14. http://linkinghub.elsevier.com/retrieve/pii/S0955221912001689.
5. Santos AM, Thomazini D, Gelfuso MV. Cold sintering and thermoelectric properties of $Ca_3Co_4O_9$ ceramics. Ceram Int. 2020 [cited 2023 Apr 19];46(9):14064-70. https://linkinghub.elsevier.com/retrieve/pii/S0272884220305319.
6. Amaveda H, Mora M, Dura OJ, Torres MA, Madre MA, Marinel S et al. Drastic enhancement of mechanical properties of $Ca_3Co_4O_9$ by B_4C addition. J Eur Ceram Soc. 2021;41(1):402-8.
7. Suwannasri W, Chueachot R, Seetawan T, Nakhowong R. Significant enhancement of the power factor in $Ca_3Co_4O_9$ by incorporating Cu_2Se. J Alloys Compd. 2021;863:158749.
8. Annamalai AR, Teja PR, Agrawal DK, Muthuchamy A. Microwave heating synthesis and thermoelectric property characterization of highly dense $Ca_3Co_4O_9$ bulk. Ceram Int. 2020;46(11 Pt A):17951-6. http://dx.doi.org/10.1016/j.ceramint.2020.04.105.
9. Miyazawa K, Amaral F, Kovalevsky AV, Graça MPF. Hybrid microwave processing of $Ca_3Co_4O_9$ thermoelectrics. Ceram Int. 2016 [cited 2023 Apr 19];42(8):9482-7. http://linkinghub.elsevier.com/retrieve/pii/S0272884216301468.
10. Dube DC, Ramesh PD, Cheng J, Lanagan MT, Agrawal D, Roy R. Experimental evidence of redistribution of fields during processing in a high-power microwave cavity. Appl Phys Lett. 2004;85(16):3632-4.
11. Yan M, Hu J. Microwave sintering of high-permeability $(Ni_{0.20}Zn_{0.60}Cu_{0.20})Fe_{1.98}O_4$ ferrite at low sintering temperatures. J Magn Magn Mater. 2006 [cited 2023 Apr 19];305(1):171-6. https://linkinghub.elsevier.com/retrieve/pii/S0304885305011686.
12. Oghbaei M, Mirzaee O. Microwave versus conventional sintering: a review of fundamentals, advantages and applications. J Alloys Compd. 2010 [cited 2024 Feb 6];494(1-2):175-89. http://linkinghub.elsevier.com/retrieve/pii/S0925838810001015.
13. Diez JC, Torres MA, Rasekh S, Constantinescu G, Madre MA, Sotelo A. Enhancement of $Ca_3Co_4O_9$ thermoelectric properties by Cr for Co substitution. Ceram Int. 2013;39(6):6051-6.
14. Schneider CA, Rasband WS, Eliceiri KW. NIH Image to ImageJ: 25 years of image analysis. Nat Methods. 2012 [cited 2023 Apr 19];9(7):671-5. http://www.nature.com/articles/nmeth.2089.
15. Machado RAM, Gelfuso MV, Thomazini D. Thermoelectric properties of barium doped calcium cobaltite obtained by simplified chemical route. Ceramica. 2021 [cited 2023 Apr 19];67(381):90-7. http://www.scielo.br/scielo.php?script=sci_arttext&pid=S0366-69132021000100090&tlng=en.
16. Delorme F, Diaz-Chao P, Guilmeau E, Giovannelli F. Thermoelectric properties of $Ca_3Co_4O_9$–Co_3O_4 composites. Ceram Int. 2015 [cited 2023 Apr 19];41(8):10038-43. http://linkinghub.elsevier.com/retrieve/pii/S0272884215008470.
17. Liu Y, Lin Y, Shi Z, Nan CW, Shen Z. Preparation of $Ca_3Co_4O_9$ and improvement of its thermoelectric properties by spark plasma sintering. J Am Ceram Soc. 2005 [cited 2012 May 21];88(5):1337-40. http://doi.wiley.com/10.1111/j.1551-2916.2005.00284.x.
18. Schulz T, Töpfer J. Thermoelectric properties of $Ca_3Co_4O_9$ ceramics prepared by an alternative pressure-less sintering/annealing method. J Alloys Compd. 2016 [cited 2023 Apr 19];659:122-6. https://linkinghub.elsevier.com/retrieve/pii/S0925838815315577.
19. Shi Z, Zhang P, Lou Z, Qin M, Xu J, Yan H et al. Grain orientation evolution and thermoelectric properties of textured $(Ca_{0.87}Ag_{0.1}La_{0.03})_3Co_4O_9$ ceramics prepared by tape casting. Ceram Int. 2021;47(6):8365-74.
20. Kingery WD, Bowen HK, Uhlmann DR. Introduction to ceramics. 2nd ed. New York: John Wiley & Sons; 1976.
21. Huang Z, Cheng J, Zhang H, Xiong Y, Zhou Z, Zheng Q et al. High-performance microwave absorption enabled by Co_3O_4 modified VB-group laminated VS_2 with frequency modulation from S-band to Ku-band. J Mater Sci Technol. 2022 [cited 2023 Mar 30];107:155-64. https://linkinghub.elsevier.com/retrieve/pii/S100503022100757X.
22. Baysinger G, Berger LI, Kehiaian HV, Roth DL, Zwillinger D, Goldberg RN et al. Physical constants of inorganic compounds. In: Lide DR, editor. CRC Handbook of Chemistry and Physics. 89th ed. Boca Raton: Taylor and Francis; 2009. p. 4-44-4-101.
23. Dudnikov VA, Fedorov AS, Orlov YS, Solovyov LA, Vereshchagin SN, Gavrilkin SY et al. Thermoelectric properties of the $SmCoO_3$ and $NdCoO_3$ cobalt oxides. Ceram Int. 2020;46(11):17987-91.

24. Presečnik M, De Boor J, Bernik S. Synthesis of single-phase $Ca_3Co_4O_9$ ceramics and their processing for a microstructure-enhanced thermoelectric performance. Ceram Int. 2016 [cited 2023 Apr 19];42(6):7315-27. https://linkinghub.elsevier.com/retrieve/pii/S0272884216001590.
25. Gunes M, Ozenbas M. Effect of grain size and porosity on phonon scattering enhancement of $Ca_3Co_4O_9$. J Alloys Compd. 2015 [cited 2023 Apr 19];626:360-7. https://linkinghub.elsevier.com/retrieve/pii/S092583881402862X.
26. Franz R, Wiedemann G. Ueber die wärme-leitungsfähigkeit der metalle. Ann Phys Chemie. 1853 [cited 2023 Apr 19];165(8):497-531. https://onlinelibrary.wiley.com/doi/10.1002/andp.18531650802.
27. Kim HS, Gibbs ZM, Tang Y, Wang H, Snyder GJ. Characterization of Lorenz number with Seebeck coefficient measurement. APL Mater. 2015;3(4):1-6. http://dx.doi.org/10.1063/1.4908244.
28. Presečnik M, Bernik S. Microstructural and thermoelectric properties of WO_3-doped $Ca_3Co_4O_9$ ceramics. Ceram Int. 2016;42(14):16103-8.
29. Wang N, Han L, He H, Ba Y, Koumoto K. Effects of mesoporous silica addition on thermoelectric properties of Nb-doped $SrTiO_3$. J Alloys Compd. 2010;497(1-2):308-11.
30. Gong C, Shi Z, Zhang Y, Chen Y, Hu J, Gou J et al. Fabrication and thermoelectric properties of Ca-Co-O ceramics with negative Seebeck coefficient. Results Phys. 2018;9:1233-8.
31. Fergus JW. Oxide materials for high temperature thermoelectric energy conversion. J Eur Ceram Soc. 2012;32(3):525-40.
32. Ling CD, Aivazian K, Schmid S, Jensen P. Structural investigation of oxygen non-stoichiometry and cation doping in misfit-layered thermoelectric $(Ca_2CoO_3\text{-}x)(CoO_2)_\delta$, $\delta \approx 1.61$. J Solid State Chem. 2007;180(4):1446-55.
33. Bresch S, Mieller B, Delorme F, Chen C, Bektas M, Moos R et al. Influence of reaction-sintering and calcination conditions on thermoelectric properties of sm-doped calcium manganate $CaMnO_3$. J Ceram Sci Technol. 2018;9(3):289-300.
34. Kenfaui D, Chateigner D, Gomina M, Noudem JG. Texture, mechanical and thermoelectric properties of $Ca_3Co_4O_9$ ceramics. J Alloys Compd. 2010 [cited 2014 Sep 18];490(1-2):472-9. http://linkinghub.elsevier.com/retrieve/pii/S0925838809020064.